RSC Advances

PAPER

View Article Online
View Journal | View Issue

Cite this: *RSC Adv.*, 2020, **10**, 25758

Thermo-driven self-assembly of a PEG-containing amphiphile in a bilayer membrane

Rui Li,†[a] Takahiro Muraoka*[b] and Kazushi Kinbara *[ab]

Received 1st May 2020
Accepted 1st July 2020

DOI: 10.1039/d0ra03920a

rsc.li/rsc-advances

Self-assembly of lipid molecules in a plasma membrane, namely lipid raft formation, is involved in various dynamic functions of cells. Inspired by the raft formation observed in the cells, here we studied thermally induced self-assembly of a synthetic amphiphile, **bola-AkDPA**, in a bilayer membrane. The synthetic amphiphile consists of a hydrophobic unit including fluorescent aromatic and aliphatic components and hydrophilic tetraethylene glycol chains attached at both ends of the hydrophobic unit. In a polar solvent, **bola-AkDPA** formed aggregates to show excimer emission. In a lipid bilayer membrane, **bola-AkDPA** showed intensified excimer emission upon increase of its concentration or elevation of the temperature; bola-type amphiphiles containing oligoethylene glycol chains likely tend to form self-assemblies in a bilayer membrane triggered by thermal stimuli.

1. Introduction

Self-assembly of lipids in a bilayer membrane, namely formation of lipid rafts, plays key roles in cellular functions,[1–10] such as signal transduction, membrane trafficking, and cell adhesion. Although lipid rafts are important and common constituents of biological membranes, development of raft-forming synthetic amphiphiles have yet to be widely demonstrated. Halogen–halogen[11–16] or aromatic–aromatic interactions[17–23] and oxidative disulfide-bond formation[24,25] have been used to promote lateral self-assembly of synthetic amphiphiles in bilayer membranes. Light-triggered raft formation was demonstrated by azobenzene-incorporated amphiphiles,[26–33] where the photoisomerization of the azobenzene unit in the hydrophobic alkyl tail from *cis* to *trans* conformers facilitates the self-assembly. In addition to the raft-formation approach by controlling the interactions at the hydrophobic portions, we recently demonstrated lateral self-assembly of a macrocyclic amphiphile induced by a thermal response of the hydrophilic octaethylene glycol (OEG) unit connecting both ends of the hydrophobic unit.[34] Upon heating, the macrocyclic amphiphile readily self-assembles, and the bilayer membrane deforms to show budding. In this study, we report a thermal response of a linear amphiphile **bola-AkDPA**, a non-cyclic pseudo-isomer of the previously-reported macrocyclic amphiphile, in a bilayer membrane (Scheme 1). The linear amphiphile **bola-AkDPA** consists of a multiblock structure incorporating hydrophilic oligoethylene glycol chains and a hydrophobic moiety connected by phosphoric ester linkages. This structure is considered to be favorable for localization of the molecules into a bilayer membrane as demonstrated by our previous studies.[34,35] To investigate the topological effect, two tetraethylene glycol (TEG) chains are attached to both ends of the hydrophobic unit, where the total number of the ethylene oxide unit is identical to that of the previous macrocyclic amphiphile.[34] A fluorescent diphenylacetylene (DPA) unit is incorporated in the hydrophobic moiety in order to detect the self-assembly by excimer emission. In the hydrophobic moiety, a (2*S*,5*S*)-hexane-2,5-diol unit conjugates the DPA-containing unit and C12 alkyl chain whose length is comparable with each other.

2. Experimental

2.1 Materials

I_2 and pivaloyl chloride were purchased from Tokyo Chemical Industry. 1.0 M tetra-*n*-butylammonium fluoride (TBAF) in tetrahydrofuran (THF) and 1.0 M triethylammonium bicarbonate (TEAB) buffer at pH 8.5 were purchased from Sigma Aldrich. $Na_2S_2O_3$ was purchased from Nacalai Tesque. Dry pyridine was purchased from Wako Pure Chemical Industries. 1,2-Dioleoyl-*sn-glycero*-3-phosphocholine (DOPC) was

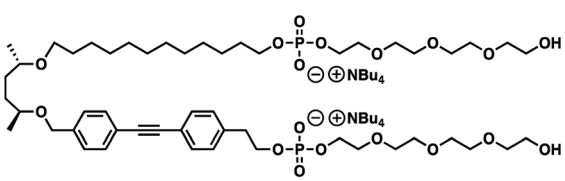

Scheme 1 Molecular structure of **bola-AkDPA**.

[a]*Institute of Multidisciplinary Research for Advanced Materials, Tohoku University, 2-1-1 Katahira, Aoba-ku, Sendai, 980-8577, Japan*

[b]*Department of Life Science and Technology, Tokyo Institute of Technology, 4259 Nagatsuta-cho, Midori-ku, Yokohama, 226-8503, Japan. E-mail: kkinbara@bio.titech.ac.jp*

† Current address of R. L. is College of Tobacco Science, Henan Agricultural University, 63 Nongye Road, Jinshui District, Zhengzhou, 450002, China.

purchased from Avanti Polar Lipids. These commercial reagents were used without further purification. Deuterated solvents were purchased from Acros Organics. Dry CH_2Cl_2 and dry THF were purchased from Kanto Chemical and passed through sequential two drying columns on a Glass-Contour system just prior to use. Deionized water (filtered through a 0.22 μm membrane filter, >18.2 MΩ cm) was purified in a Milli-Q system of Millipore. Silica gel column chromatography was carried out with Chromatorex DIOL silica (MB100-75/200, spherical, neutral, particle size: 75–200 μm, pore size: 10 nm) purchased from Fuji Silysia Chemical.

2.2 Instrumentation

^{1}H and ^{13}C nuclear magnetic resonance (NMR) spectra were recorded on 400 MHz FT NMR Bruker BioSpin AVANCE III 400 spectrometer, where the chemical shifts were determined with respect to tetramethylsilane (TMS). Dynamic light scattering (DLS) measurements were performed with Malvern Zetasizer Nano ZSP light-scattering detector, where a low-volume quartz batch cuvette (ZEN2112) was used. Matrix assisted laser desorption/ionization-time of flight mass (MALDI-TOF MS) measurements were performed with Bruker autoflex speed mass spectrometer with gentisic acid (GA) as a matrix. UV absorption spectra were recorded on JASCO V-530 UV-Vis spectrophotometer. Fluorescence spectra were recorded on JASCO FP-6500 spectrofluorometer. Fluorescence lifetime was measured with Hamamatsu Photonics Quantaurus-Tau fluorescence lifetime spectrometer. Fluorescent and phase-contrast microscopic observations were performed with BX-51 microscope (Olympus, Tokyo, Japan), where U-MWU2 mirror unit (Excitation filter: 330–385 nm, emission filter: 420 nm, dichroic mirror: 400 nm) was used for fluorescence observation and Olympus UPLFLN 100XO2PH (magnification: ×100 and ×160) was attached as the objective lens. Surface tension was measured with Kyowa Interface Science Contact Angle Meter DMe-201 by a sessile drop method.

2.3 Synthesis of bola-AkDPA

To a dry pyridine (8 mL) solution of **1**[34] (40.0 mg, 0.0745 mmol) and **2**[35] (117 mg, 0.228 mmol) was added pivaloyl chloride (0.20 mL, 1.1 mmol) at 0 °C under Ar, and the resulting mixture was stirred for 1 h at 0 °C in the dark (Scheme 2). To the resulting mixture was added a solution of I_2 (250 mg, 0.985 mmol) in a mixture of pyridine (3 mL) and water (1 mL), followed by the addition of saturated $Na_2S_2O_3$ aqueous solution (4 mL) and 1.0 M TEAB buffer (7 mL). The reaction mixture was evaporated to dryness under reduced pressure at 30 °C. To the residue was added CH_2Cl_2 (20 mL), and the resulting mixture was filtered off from insoluble substances and evaporated to dryness under reduced pressure at 30 °C. The residue was chromatographed on silica gel to allow isolation of a product, in which the terminal hydroxy groups of the tetraethylene glycol chains were protected by triisopropylsilyl groups. To a dry THF (10 mL) solution of the obtained product (77.1 mg, 0.0566 mmol) was added 1.0 M THF solution of TBAF (0.56 mL, 0.56 mmol) at 0 °C under Ar, and the resulting mixture was stirred for 2 h at room temperature. Then, to the reaction mixture was added 1.0 M TEAB buffer (4 mL). After being stirred for 20 min at 0 °C, the resulting mixture was evaporated to dryness under reduced pressure at 30 °C, and the residue was chromatographed on silica gel to isolate **bola-AkDPA** in 17% yield (20.0 mg, 0.0130 mmol) as yellowish oil. ^{1}H NMR (400 MHz, $CDCl_3$ containing 0.03% TMS, 23 °C): δ 7.47 (d, J = 8.0 Hz, 2H), 7.41 (d, J = 8.0 Hz, 2H), 7.32 (d, J = 8.0 Hz, 2H), 7.25 (m, 2H), 4.61 (d, J = 12.8 Hz, 1H), 4.43 (d, J = 12.6 Hz, 1H), 4.12–3.43 (m, 40H), 3.26 (m, 16H), 2.97 (m, 2H), 1.63 (m, 16H), 1.42 (m, 16H), 1.26–1.10 (m, 30H), 0.99 (t, J = 7.2 Hz, 24H) ppm; ^{13}C NMR (100 MHz, $CDCl_3$, 23 °C): δ 139.32, 131.51, 129.29, 127.50, 122.37, 120.96, 89.44, 88.97, 75.18, 75.04, 72.75, 70.79–70.33, 69.89, 68.54, 65.88, 64.87–64.51, 61.47, 58.71, 37.09, 32.30, 30.80, 30.24, 29.81, 29.62, 27.21, 26.38, 25.90, 23.97, 19.73, 19.63, 13.77 ppm; MALDI-TOF MS (GA, reflector negative mode):m/z: calculated for $C_{51}H_{84}NaO_{18}P_2$: 1069.5042 $[M - 2NBu_4 + Na]^-$; found: 1069.5639.

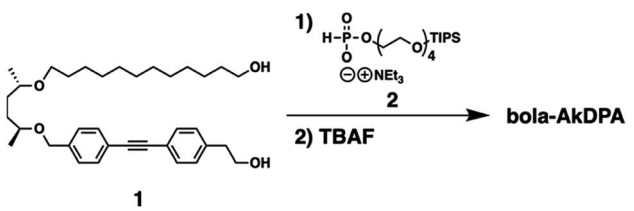

Scheme 2 Synthetic scheme of bola-AkDPA.

2.4 Preparation of giant unilamellar vesicles (GUVs)

To a test tube was added $CHCl_3$ solutions of **bola-AkDPA** (1.0 mM, 4 μL) and DOPC (1.0 mM, 36 μL), which was gently evaporated by Ar flow. The resulting thin film on the bottom of the test tube was further dried under vacuum for 4 h at 25 °C, to which was added HEPES buffer (20 mM, 100 μL, pH 7.45) containing 200 mM sucrose. Then, the mixture was incubated for 10 h at 37 °C. For the phase-contrast microscopic observations, HEPES buffer (20 mM, 100 μL, pH 7.45) containing 200 mM glucose was added to the GUV suspension to enhance the contrast between the inside and outside of the GUVs by a large difference in the refractive indices.

2.5 Preparation of large unilamellar vesicles (LUVs)

To a test tube was added $CHCl_3$ solutions of **bola-AkDPA** (1.0 mM, 5 μL) and DOPC (1.0 mM, 45 μL) as well as a mixture of $CHCl_3$ and MeOH (2 : 1 v/v, 50 μL), and the resulting mixture was gently evaporated by Ar flow. The resulting thin film on the bottom of the test tube was further dried under vacuum for 1.5 h at 25 °C, to which was added HEPES buffer (20 mM, 1.0 mL, pH 7.45). Then, the mixture was shaken on a shaker at 200 min^{-1} for 1 h at 37 °C, followed by freezing-and-thawing for three times, vortex mixing for 10 s and incubation at 37 °C for 10 h. Finally, the mixture was passed through a polycarbonate membrane (200 nm pore size) attached to a LiposoFast-Basic device by pushing the sample back and forth between the two gastight syringes over 13 times.

3. Results and discussion

3.1 Self-assembly of bola-AkDPA in THF and water

Synthetic bola-amphiphile, **bola-AkDPA**, consists of a hydrophobic DPA and an aliphatic unit connected with two TEG chains *via* phosphoester groups as hydrophilic units. Because of the amphiphilic structure, it was expected that **bola-AkDPA** self-assembles in polar solvents. Dynamic light scattering measurement showed that **bola-AkDPA** was soluble in an organic solvent such as tetrahydrofuran (THF), while it formed aggregates in water ([**bola-AkDPA**] = 50 μM, mean hydrodynamic diameter: 80 nm, Fig. 1a). Surface tension change of the aqueous solution upon increase in the concentration of **bola-AkDPA** levelled off above 45 μM; the critical aggregation concentration of **bola-AkDPA** was evaluated to be 45 μM (Fig. 1b). The absorption bands of **bola-AkDPA** slightly blue-shifted in water from that in THF, suggesting H-aggregation of the DPA unit (289 and 307 nm in THF, 287 and 305 nm in water; Fig. 1c).[36–38] The self-assembly of **bola-AkDPA** encouraged by water can also be monitored by fluorescence (excitation at 288 nm, Fig. 1d). In THF, **bola-AkDPA** showed emission bands at 312, 324 and 333 nm, corresponding to the fluorescence of the monomeric DPA unit. Upon increasing the water ratio, the intensity of the fluorescence at 381 nm enhanced, and became dominant in water. The lifetime of the 380 nm fluorescence was 3.41 ns, suggesting excimer fluorescence (Fig. 1e),[39,40] also indicating self-assembly of **bola-AkDPA** (Fig. 1d blue line), in consistent with the result of DLS (Fig. 1a blue line).

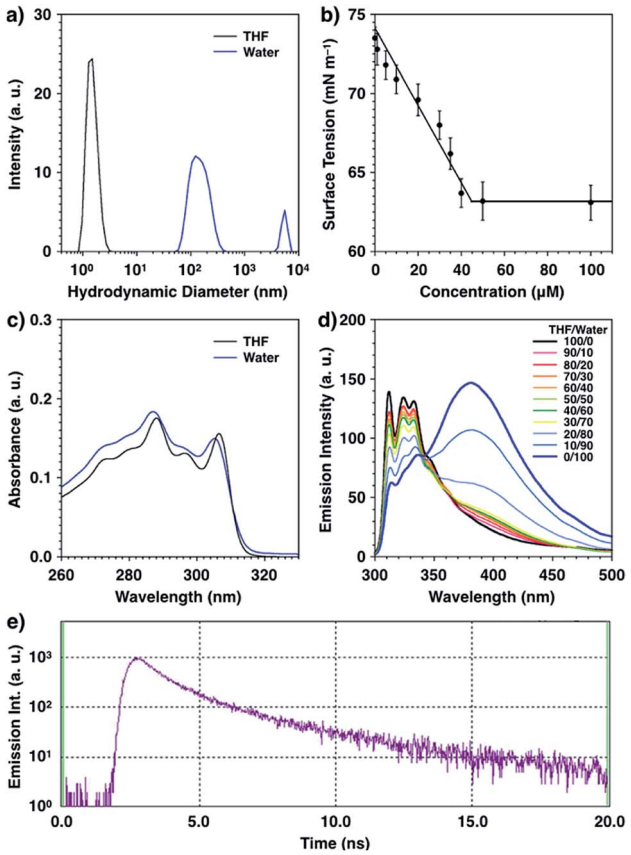

Fig. 1 (a) DLS size distribution profiles of **bola-AkDPA** in THF (black) and water (blue) at 50 μM at 20 °C. (b) Concentration-dependent surface tension changes of **bola-AkDPA** in water at 20 °C. (c) UV absorption spectra of **bola-AkDPA** in THF (black) and water (blue) at 50 μM at 20 °C. (d) Fluorescence spectra of **bola-AkDPA** in mixtures of THF and water at varying ratios at 50 μM at 20 °C. Excitation: 288 nm. (e) Fluorescence intensity decay profile of **bola-AkDPA** in water at 20 °C. Excitation: 280 nm, emission: 380 nm. [**bola-AkDPA**] = 50 μM.

3.2 Self-assembly of bola-AkDPA in bilayer membrane

GUVs consisting of DOPC and **bola-AkDPA** ($GUVs_{DOPC\cdot bola\text{-}AkDPA}$) were prepared by the gentle hydration method as described in the Experimental section, which were visualized by phase-contrast microscopy in HEPES buffer ([DOPC]/[**bola-AkDPA**] = 90/10, Fig. 2a). Under fluorescence microscopic observation, the $GUVs_{DOPC\cdot bola\text{-}AkDPA}$ showed ring images, suggesting incorporation of **bola-AkDPA** in the DOPC bilayer (Fig. 2b). Meanwhile, by extrusion of the lipids through a polycarbonate membrane, LUVs consisting of DOPC and **bola-AkDPA** ($LUVs_{DOPC\cdot bola\text{-}AkDPA}$) with different ratios were prepared in HEPES buffer ([DOPC]/[**bola-AkDPA**] = 99/1 and 90/10). DLS measurement indicated the mean hydrodynamic diameter of the $LUVs_{DOPC\cdot bola\text{-}AkDPA}$ to be 151 nm (99/1) and 142 nm (90/10) with monodisperse size distribution profiles (Fig. 3a and d blue lines). Upon excitation at 288 nm at 20 °C, $LUVs_{DOPC\cdot bola\text{-}AkDPA}$(99/1) showed fluorescence bands corresponding to the monomeric DPA unit almost dominantly (313, 325 and 334 nm; Fig. 3b blue solid line), suggesting **bola-AkDPA** was mostly dispersed in the DOPC bilayer. Interestingly, $LUVs_{DOPC\cdot bola\text{-}AkDPA}$(90/10) containing an increased concentration of **bola-AkDPA** showed a fluorescent spectrum with a largely different profile from $LUVs_{DOPC\cdot bola\text{-}AkDPA}$(99/1). Namely, in addition to the monomer emission bands of the DPA unit, the excimer emission was also observed around 380 nm as a shoulder (Fig. 3e blue solid line). Thus, **bola-AkDPA** likely forms self-assemblies in the DOPC bilayer membrane upon increase in its concentration.

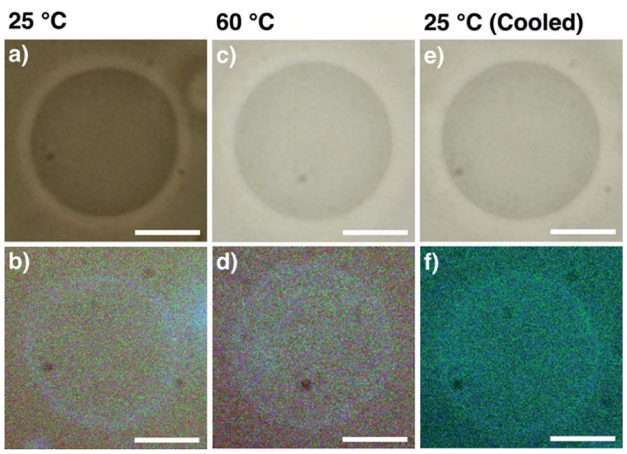

Fig. 2 Phase-contrast (a, c and e) and fluorescence (b, d and f) micrographs of GUVs consisting of DOPC and **bola-AkDPA** in HEPES buffer at (a and b) 25, (c and d) 60 (heated), and (e and f) 25 °C (cooled). [DOPC]/[**bola-AkDPA**] = 90/10. [DOPC] + [**bola-AkDPA**] = 200 μM. Scale bars: 5.0 μm.

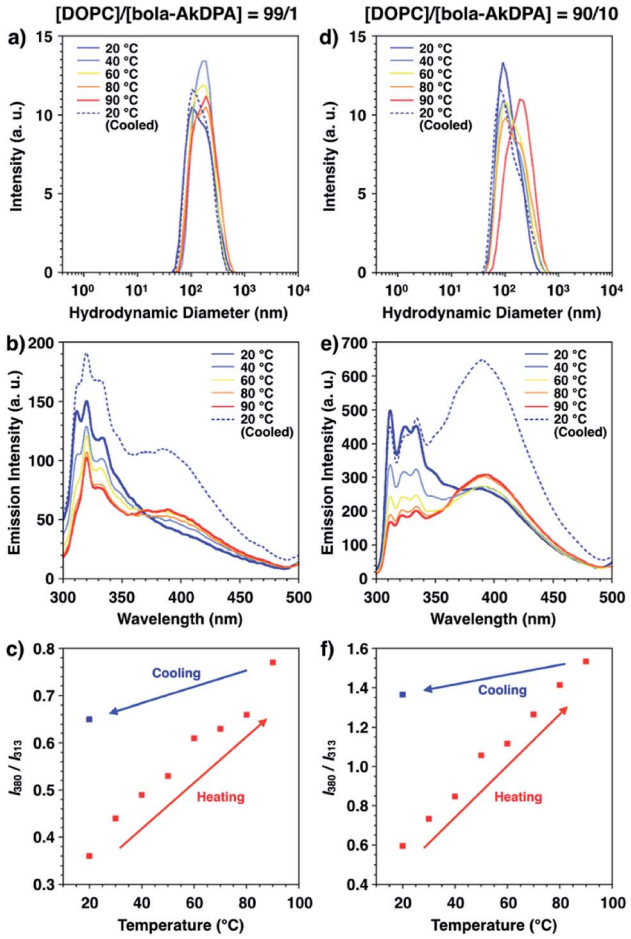

Fig. 3 (a and d) DLS size distribution profiles, (b and e) fluorescence spectra and (c and f) temperature dependent I_{380}/I_{313} changes of $LUVs_{DOPC\cdot bola\text{-}AkDPA}$ in HEPES buffer. [DOPC]/[**bola-AkDPA**] = (a–c) 99/1 and (d–f) 90/10. Red and blue arrows in (c and f) represent the directions of I_{380}/I_{313} changes in the heating and cooling processes, respectively. [DOPC] + [**bola-AkDPA**] = 50 μM.

Interestingly, the fluorescence profiles also changed upon temperature elevation. In the temperature elevation process from 20 °C to 90 °C, the excimer emission of $LUVs_{DOPC\cdot bola\text{-}AkDPA}$(99/1) intensified, while the intensities of the monomer emission bands decreased (Fig. 3b red line). As shown in Fig. 3c, the ratio between the intensities of the emission bands at 380 nm (I_{380}, excimer emission) and 313 nm (I_{313}, monomer emission), I_{380}/I_{313}, enhanced monotonically in the heating process from 20 to 90 °C (I_{380}/I_{313} = 0.36 at 20 °C, 0.77 at 90 °C). Furthermore, after cooling to 20 °C, the ratio I_{380}/I_{313} did not return to the original value; I_{380}/I_{313} at 20 °C after cooling was significantly higher than that before heating (I_{380}/I_{313} = 0.65 at 20 °C after cooling). DLS profiles displayed the essentially unchanged size and distribution pattern through the temperature changing processes (Fig. 3a). Importantly, $LUVs_{DOPC\cdot bola\text{-}AkDPA}$(90/10) also showed analogous spectral change to that of $LUVs_{DOPC\cdot bola\text{-}AkDPA}$(99/1) exhibiting an enhancement of the excimer emission intensity and decrease in the intensities of the monomer emission bands upon heating (Fig. 3e). Indeed, I_{380}/I_{313} increased upon heating followed by a hysteretic spectral change upon cooling to preserve a significantly higher I_{380}/I_{313} value at 20 °C compared to that before heating (I_{380}/I_{313} = 0.59 at 20 °C, 1.53 at 90 °C and 1.37 at 20 °C after cooling; Fig. 3f). These results suggest the self-assembly of **bola-AkDPA** promoted by heating. As reported previously, an oligoethylene glycol chain responses to temperature elevation to increase the hydrophobicity by a conformational change.[41–49] Such a thermal response of the TEG chains in **bola-AkDPA** to increase the hydrophobicity likely promotes the self-assembly in a bilayer membrane. Under the optical microscopic observations of $GUVs_{DOPC\cdot bola\text{-}AkDPA}$(90/10), fluorescent domain formation was not observed during heating and cooling processes between 25 and 60 °C, and the spherical morphology of the GUV was essentially unchanged without showing budding or membrane deformation (Fig. 2c–f). Thus, it is considered that size of the domain formed by **bola-AkDPA** in the membrane is as small as sub-μm or nm scale. In our previous paper, it is demonstrated that, upon heating, a cyclic-pseudo-isomer of **bola-AkDPA** forms a microscopically-observable μm-scale domain in a membrane, which promotes membrane budding.[34] Thus, while incorporation of oligoethylene glycol moieties into the amphiphiles is likely to be effective to promote the thermally-induced self-assembly in a membrane, the topological difference of the molecular structures would largely influence the physical properties, such as size and curvature, of the self-assembled domains. For better understanding of the topological effects, detailed characterization of the conformations, packing and dynamics of the oligoethylene glycol-containing amphiphiles in a membrane is under investigation.

4. Conclusions

Inspired by the self-assembly of lipid molecules in a plasma membrane observed in the cells, we reported thermally induced self-assembly of a synthetic amphiphile, **bola-AkDPA**, in a bilayer membrane. Upon increasing the solvent polarity, **bola-AkDPA** formed aggregates to show excimer emission from the hydrophobic aromatic unit. In a lipid bilayer membrane, **bola-AkDPA** showed intensified excimer emission upon increase of its concentration or elevation of the temperature, indicating self-assembly. Microscopic observations suggested that the size of the self-assembly is as small as sub-μm or nm-scale, and essentially no morphological changes of the membranes were observed after the formation of the aggregates. Our previous study demonstrated that a cyclic pseudo-isomer formed μm-scale self-assembly in a membrane upon heating, which further promoted budding.[34] Thus, it could be demonstrated that oligoethylene glycol-containing amphiphiles tend to form self-assembly in a bilayer membranes upon temperature elevation, where the topology of the molecule likely influences the physical properties of the self-assembly significantly.

Conflicts of interest

There are no conflicts to declare.

Acknowledgements

This work was partially supported by Grant-in-Aids for Scientific Research on Innovative Areas "Molecular Engine (No. 8006)" (18H05419 to KK) and "π-System Figuration (No. 2601)" (26102001 to TM), Scientific Research B (16H04129 to KK, 19H02828 to TM) and the Management Expenses Grants for National Universities Corporations from MEXT, Japan.

Notes and references

1 K. Simons and E. Ikonen, *Nature*, 1997, **387**, 569–572.
2 D. A. Brown and E. London, *Annu. Rev. Cell Dev. Biol.*, 1998, **14**, 111–136.
3 L. J. Pike, *Biochem. J.*, 2004, **378**, 281–292.
4 D. Lingwood and K. Simons, *Science*, 2009, **327**, 46–50.
5 S. Staubach and F.-G. Hanisch, *Expert Rev. Proteomics*, 2011, **8**, 263–277.
6 M. L. Kraft, *Mol. Biol. Cell*, 2013, **24**, 2765–2768.
7 A. Laurenzana, G. Fibbi, A. Chillà, G. Margheri, T. Del Rosso, E. Rovida, M. Del Rosso and F. Margheri, *Cell. Mol. Life Sci.*, 2015, **72**, 1537–1557.
8 J. H. Lorent and I. Levental, *Chem. Phys. Lipids*, 2015, **192**, 23–32.
9 F. Mollinedo and C. Gajate, *Adv. Biol. Regul.*, 2015, **57**, 130–146.
10 I. Levental and S. L. Veatch, *J. Mol. Biol.*, 2016, **428**, 4749–4764.
11 R. Elbert, T. Folda and H. Ringsdorf, *J. Am. Chem. Soc.*, 1984, **106**, 7687–7692.
12 R. J. Mart, K. P. Liem, X. Wang and S. J. Webb, *J. Am. Chem. Soc.*, 2006, **128**, 14462–14463.
13 S. J. Webb, K. Greenaway, M. Bayati and L. Trembleau, *Org. Biomol. Chem.*, 2006, **4**, 2399–2407.
14 G. T. Noble, F. L. Craven, J. Voglmeir, R. Šardzík, S. L. Flitsch and S. J. Webb, *J. Am. Chem. Soc.*, 2012, **134**, 13010–13017.
15 G. T. Noble, F. L. Craven, M. D. Segarra-Maset, J. E. R. Martínez, R. Šardzík, S. L. Flitsch and S. J. Webb, *Org. Biomol. Chem.*, 2014, **12**, 9272–9278.
16 F. L. Craven, J. Silva, M. D. Segarra-Maset, K. Huang, P. Both, J. E. Gough, S. L. Flitsch and S. J. Webb, *Chem. Commun.*, 2018, **54**, 1347–1350.
17 D. Y. Sasaki, D. R. Shnek, D. W. Pack and F. H. Arnold, *Angew. Chem., Int. Ed.*, 1995, **34**, 905–907.
18 C. Goto, M. Yamamura, A. Satake and Y. Kobuke, *J. Am. Chem. Soc.*, 2001, **123**, 12152–12159.
19 N. Sakai, J. Mareda and S. Matile, *Acc. Chem. Res.*, 2005, **38**, 79–87.
20 H. Siu, J. Duhamel, D. Y. Sasaki and J. L. Pincus, *Langmuir*, 2010, **26**, 10985–10994.
21 T. Muraoka, T. Shima, T. Hamada, M. Morita, M. Takagi and K. Kinbara, *Chem. Commun.*, 2011, **47**, 194–196.
22 T. Muraoka, T. Shima, T. Hamada, M. Morita, M. Takagi, K. V. Tabata, H. Noji and K. Kinbara, *J. Am. Chem. Soc.*, 2012, **134**, 19788–19794.
23 T. Muraoka and K. Kinbara, *Chem. Commun.*, 2016, **52**, 2667–2678.
24 J. D. Hartgerink, *Curr. Opin. Chem. Biol.*, 2004, **8**, 604–609.
25 Z. Lin, L. Li, Y. Yang, H. Zhan, Y. Hu, Z. Zhou, J. Zhu, Q. Wang and J. Deng, *Org. Biomol. Chem.*, 2013, **11**, 8443–8451.
26 H. Fujiwara and Y. Yonezawa, *Nature*, 1991, **351**, 724–726.
27 M. Tanaka, T. Sato and Y. Yonezawa, *Langmuir*, 1995, **11**, 2834–2836.
28 Y. Lei and J. K. Hurst, *Langmuir*, 1999, **15**, 3424–3429.
29 K. Yasuhara, Y. Sasaki and J. Kikuchi, *Colloid Polym. Sci.*, 2008, **286**, 1675–1680.
30 T. Hamada, R. Sugimoto, T. Nagasaki and M. Takagi, *Soft Matter*, 2011, **7**, 220–224.
31 D. M. C. Ramirez, S. P. Pitre, Y. A. Kim, R. Bittman and L. J. Johnston, *Langmuir*, 2013, **29**, 3380–3387.
32 J. A. Frank, H. G. Franquelim, P. Schwille and D. Trauner, *J. Am. Chem. Soc.*, 2016, **138**, 12981–12986.
33 P. Urban, S. D. Pritzl, D. B. Konrad, J. A. Frank, C. Pernpeintner, C. R. Roeske, D. Trauner and T. Lohmüller, *Langmuir*, 2018, **34**, 13368–13374.
34 R. Li, T. Muraoka and K. Kinbara, *Chem. Commun.*, 2017, **53**, 11662–11665.
35 T. Muraoka, T. Endo, K. V. Tabata, H. Noji, S. Nagatoishi, K. Tsumoto, R. Li and K. Kinbara, *J. Am. Chem. Soc.*, 2014, **136**, 15584–15595.
36 F. Nüesch and M. Grätzel, *Chem. Phys.*, 1995, **193**, 1–17.
37 J. M. Lim, P. Kim, M.-C. Yoon, J. Sung, V. Dehm, Z. Chen, F. Würthner and D. Kim, *Chem. Sci.*, 2013, **4**, 388–397.
38 V. Karunakaran, D. D. Prabhu and S. Das, *J. Phys. Chem. C*, 2013, **117**, 9404–9415.
39 B. Brocklehurst, D. C. Bull, M. Evans, P. M. Scott and G. Stanney, *J. Am. Chem. Soc.*, 1975, **97**, 2977–2978.
40 M. Wierzbicka, I. Bylińska, C. Czaplewski and W. Wiczk, *RSC Adv.*, 2015, **5**, 29294–29303.
41 H. Matsuura and T. Miyazawa, *J. Polym. Sci., Part A-1: Polym. Chem.*, 1969, **7**, 1735–1744.
42 S. Saeki, N. Kuwahara, M. Nakata and M. Kaneko, *Polymer*, 1976, **17**, 685–689.
43 H. Matsuura and K. Fukuhara, *J. Mol. Struct.*, 1985, **126**, 251–260.
44 M. Björling, G. Karlström and P. Linse, *J. Phys. Chem.*, 1991, **95**, 6706–6709.
45 T. Muraoka, K. Adachi, M. Ui, S. Kawasaki, N. Sadhukhan, H. Obara, H. Tochio, M. Shirakawa and K. Kinbara, *Angew. Chem., Int. Ed.*, 2013, **52**, 2430–2434.
46 S. Kawasaki, T. Muraoka, H. Obara, T. Ishii, T. Hamada and K. Kinbara, *Chem.–Asian J.*, 2014, **9**, 2778–2788.
47 N. Sadhukhan, T. Muraoka, D. Abe, Y. Sasanuma, D. R. G. Subekti and K. Kinbara, *Chem. Lett.*, 2014, **43**, 1055–1057.
48 S. Kawasaki, T. Muraoka, T. Hamada, K. Shigyou, F. Nagatsugi and K. Kinbara, *Chem.–Asian J.*, 2016, **11**, 1028–1035.
49 R. Li, T. Muraoka and K. Kinbara, *Langmuir*, 2016, **32**, 4546–4553.

